Power System Technology
ISSN:1000-3673

Received: 16-01-2024 *Revised: 12-02-2024* *Accepted: 07-03-2024*

NO_X Emission Prediction of a dual-fuel (Diesel + CNG) Compression Ignition Engine Using the DCNN model

[1]Yasser Niknam, [2]Davood Mohammad Zamani[*], [3]Mohammad Gholami Pareshkoohi
[1]Department of Biosystems Engineering, Takestan Branch, Islamic Azad University, Takestan, Iran
yasser18niknam@gmail.com
[2]Department of Biosystems Engineering, Takestan Branch, Islamic Azad University, Takestan, Iran
mdzamani@iau.ac.ir
[3]Department of Mechanical Engineering, Shahr-e-Qods Branch, Islamic Azad University, Tehran, Iran
Mohammad.gholami@iau.ac.ir

***Abstract*—** One of the viable solutions for utilizing natural gas in diesel engines involves adopting dual-fuel technology. This study converted the MT440C Compression Ignition (CI) engine into a dual-fuel engine, combining Diesel and Compressed Natural Gas (CNG) as its primary fuel. This investigation aims to assess the impact of natural gas as the primary fuel and diesel fuel as the spark ignition source on a 4-cylinder CI engine to reduce diesel fuel consumption. To address the challenge of accurately predicting Nitrogen Oxide (NO_X) emissions from a dual-fuel Compression Ignition Engine (utilizing Diesel and CNG) under transient operating conditions, a NO_X reduction prediction model is proposed based on the Deep Convolutional Neural Network (DCNN) architecture. Convolutional Neural Networks (CNNs) represent a more intricate class of neural networks than conventional artificial neural networks. The primary advantage of CNNs, owing to their deep architecture, lies in their capability to discern and extract distinct and heterogeneous features at various levels of abstraction. The experimental data utilized in this study were gathered from the Engine Research Center of Tabriz Motorsazan Company in Iran. Experiments were conducted under stable conditions at engine speeds of 1200, 1400, 1600, 1800, and 2000 revolutions per minute (rpm). Each experimental run was repeated three times to ensure comprehensive data collection. To effectively predict NO_X emissions from the dual-fuel engine during training, the proposed DCNN initially extracts features from multidimensional data and subsequently employs these features to establish the relationships between different time steps. The experimental results demonstrate that the proposed DCNN model exhibits superior accuracy, convergence, and robustness in predicting transient NO_X emissions from the dual-fuel engine. This is evident through a root mean square error (RMSE) of 21.70 and a fitting coefficient (R2) of 0.997, affirming the high precision and effectiveness of the proposed DCNN model in managing multidimensional time-series datasets.

Keywords: DCNN Model, The Dual-fuel Engine, CI Engine, NO_X Emissions, CNN, LSTM.

Power System Technology
ISSN:1000-3673

Received: 16-01-2024 *Revised: 12-02-2024* *Accepted: 07-03-2024*

I. INTRODUCTION

Today, the world is facing an energy resource crisis, with limited fossil fuel resources (hydrocarbons) unable to meet the growing energy demand [1]. This issue is compounded by the rising prices of fossil fuels and environmental pollution, which encourages researchers to seek alternative energy sources that are renewable, safe, and environmentally friendly [2]. Currently, diesel engines, which play a fundamental role in providing power for both road and off-road vehicles, are considered one of the primary consumers of fossil fuels. These engines significantly contribute to acoustic and environmental pollution [3]. The use of various fuels in diesel engines has led to the utilization of dual-fuel diesel engines [4]. One of the critical features of dual-fuel diesel engines is the combination of gas-diesel combustion, which reduces emissions and lowers fuel consumption. Diesel engines have diverse applications in industries and agriculture [5]. Their deployment in various conditions has prompted extensive research on this engine category.

The complexity of the ignition phenomenon and the challenges related to emissions pollution have led researchers to focus on the performance parameters and emission characteristics of diesel engines [6]. Today, dual-fuel diesel engines have become instrumental in improving ignition quality performance parameters and reducing emissions pollution [7]. One of the gaseous fuels capable of being used in dual-fuel diesel engines is Compressed Natural Gas (CNG) [8]. Due to environmental regulations, the detrimental effects of environmental pollutants, the high cost of processing conventional fuels such as diesel and gasoline, and the abundant availability and cost-effectiveness of natural gas in a country like Iran, which possesses rich natural gas resources, have garnered significant attention and research interest [9]. In Spark Ignition (SI) engines, natural gas is readily usable due to the ignition of the fuel-air mixture through SI [10]. However, in Compression Ignition (CI) engines, due to the high-octane rating of natural gas and the absence of SI, self-ignition of natural gas requires high compression ratios [11]. Using natural gas as a fuel in SI engines has undergone years of research and development, and it is currently extensively employed in internal combustion engines in some countries, including Iran.

Nevertheless, applying natural gas as a fuel in CI engines without implementing an ignition system is still in the research phase and has not yet reached industrialization [12]. Due to their lower compression ratio, replacing gasoline fuel with natural gas is feasible in ignition spark or, colloquially, gasoline engines. Considering that due to the high-octane number of natural gas (methane's octane number is approximately 130, while gasoline without lead has an octane number of around 85), a SI will still be required for the air-gas mixture. Furthermore, due to the relatively low compression ratio of such engines (between 8 and 13), it is possible to safely substitute gasoline with gas with minor modifications to the engine [13]. However, it is impossible for CI engines to fully substitute diesel fuel (gasoline) with gas because they lack an electric SI system and rely on high-pressure diesel fuel injection into the compressed air to initiate ignition. Therefore, even under optimal conditions, a dual-fuel CI engine will need a precise percentage of diesel fuel injection into the compressed gas and air mixture. Among the challenges associated with using natural gas as a fuel in standard CI engines, the high cost of converting these engines into SI engines is noteworthy [14]. This transformation necessitates using ignition system components such as coil, Delco, wire, and spark plugs in electronic fuel injection systems, processors, and related sensors, and cylinder modifications and spark plug installation are relatively challenging tasks [15].

Power System Technology
ISSN:1000-3673
Received: 16-01-2024 Revised: 12-02-2024 Accepted: 07-03-2024

Diesel fuel, when compared to other fuels usable in CI engines, possesses a lower cetane number (CN), lower well-to-wheels energy consumption, and relatively low CO and HC emissions. However, its well-to-wheels emissions of Nitrogen Oxide (NO_X) and particulate matter are high. CN is a relative measurement of the time delay between fuel injection into the combustion chamber and the start of combustion [16]. The well-to-wheel ratio is also a method for analyzing cycle-based engine life [17]. Given that the molecular formula of CNG is more straightforward than that of diesel and its combustion cycle is complete, it emits fewer CO and HC pollutants. Reasons for increased NO_X can be attributed to high combustion temperatures, thermal concentration in the combustion chamber, and improper engine cooling.

Earlier studies have focused on the feasibility of using CNG in CI engines, and the effects of employing this blended fuel on engine performance and emissions of pollutants have been examined [18]. This study uses a DCNN model to predict NO_X emissions in dual-fuel CI engines. Convolutional Neural Networks (CNNs) are deep models that employ replaceable filters and local combination operations successively applied to raw input values, generating hierarchical layers of intricate features [19].

CNNs typically consist of numerous interconnected convolutional and pooling layers [20]. The primary strength of CNN architecture lies in its ability to extract distinctive and non-uniform features at various abstraction levels. Another characteristic of CNNs is their capability to capture nonlinear relationships between inputs and outputs [21]. Features such as local connections, weight sharing, and pooling empower CNNs to capture the spatial features of data [22] effectively.

Consequently, when confronted with spatial correlations among control parameters of diesel engines, CNNs can efficiently extract pertinent feature information. Currently, obtaining the primary map of NO_X emissions through extensive Calibration Tests is being conducted, which, due to the high cost of NO_X sensors, is both time-consuming and requires significant investment [23]. Therefore, achieving a straightforward method for predicting NO_X emissions in CI engines is more important than ever. Predictive methods based on physical models can be employed to estimate NO_X emissions in steady-state conditions. However, accurately predicting NO_X emissions under transient conditions due to rapid changes in the speed of CI engines, torque, and the injection of various fuel blends presents various challenges. In light of these challenges, a DCNN-based model is proposed to enhance the accuracy of NO_X emissions prediction in dual-fuel CI engines.

The proposed model initially leverages the spatial data extraction capabilities of CNN to generate a set of valuable features and then utilizes the temporal pattern recognition capabilities of Long Short-Term Memory (LSTM) by incorporating these features to complete the training process. Consequently, the possibility of a comprehensive analysis of transient emissions data and precise representation of the nonlinear dynamics associated with transient emissions in dual-fuel CI engines is provided. The objective of presenting the proposed DCNN model is to increase the accuracy of NO_X emissions prediction. This study considers the recorded values for the NO_X emissions variable from a dual-fuel CI engine, including emissions time series. The proposed DCNN model can extract features from this data and enhance prediction accuracy.

Section III presents the Proposed Method of this paper, which explains the data set, data preprocessing, CNN, LSTM, and the proposed DCNN model. The experimental results, which involve experimental equipment and schema, simulation environment, evaluation criteria, and

Power System Technology
ISSN:1000-3673
Received: 16-01-2024 Revised: 12-02-2024 Accepted: 07-03-2024

output results, are discussed in section IV. Finally, conclusions and future works are presented in section V.

II. RELATED WORKS

In the ever-evolving landscape of technology and industry, neural networks and artificial intelligence (AI) play pivotal roles in addressing various challenges. From spam detection leveraging evolutionary data mining systems to noise reduction techniques applied in medical imaging using wavelet and neural networks, the integration of AI solutions continues to advance across diverse sectors. In this introduction, we delve into a selection of innovative studies encompassing supply chain risk management, material requirements planning with fuzzy modeling, and the application of AI-driven approaches in predicting corporate financial crises. Through these examples, we explore the transformative impact of neural networks and AI on solving real-world industrial problems [24-29].

In recent years, deep learning techniques have significantly increased in various fields. The algorithms employed in deep learning have found extensive applications in predicting transient pollutants such as NO_X in diesel engines. This section examines some studies conducted in the field of NO_X emissions prediction using deep learning.

In [30] 2023, a combination of CNN and LSTM models was utilized to predict the NO_X levels under transient conditions on a diesel engine model D25TCIF. The proposed model in this study was trained and verified on data collected during a thermal cycle corresponding to the World Harmonized Transient Cycle (WHTC) test. The model's accuracy was evaluated based on the results, yielding two performance metrics: RMSE = 35.6 and $R^2 = 0.97$.

In [31] 2022, a Deep Neural Network (DNN) was employed to predict the NO_X output levels from heavy-duty vehicles in two states: engine-out and tailpipe emissions. The proposed model in this study was tested and verified using a dataset obtained through dynamometer measurements. The model's accuracy was assessed using the R^2 criterion, yielding values of 0.92-0.95 based on the results obtained for engine-out and tailpipe emissions.

In [32] 2022, a one-dimensional Convolutional Neural Network (1D-CNN) model was utilized to predict NO_X levels and computation times. The proposed 1D-CNN model was tested and verified using data from a 500MW coal-fired power plant. The model's accuracy, as determined by the RMSE criterion, was 70.6.

In [33] 2021, an LSTM model was employed to predict instantaneous NO_X emissions in a diesel engine. The data used in this study was collected using Complete Ensemble Empirical Mode Decomposition with Adaptive Noise (CEEMDAN) for testing and verifying the LSTM model. Based on the results obtained, the model's accuracy was evaluated using two criteria: RMSE = 46.11 and $R^2 = 0.98$.

In [34] 2020, a CNN model was utilized to predict NO_X emissions from a coal-fired boiler. The proposed model in this study was tested and verified using data collected from a 330 MW power plant boiler operating in conjunction with coal-fired processes. The model's accuracy was assessed based on the results, yielding an evaluation metric of RMSE = 68.

In [35] the year 2020, a combination of two models, CNN and LSTM, was employed to predict NO_X levels in a Fluid Catalytic Cracking (FCC) unit. The proposed model in this research was tested and verified using data gathered from a Distributed Control System (DCS) within a refinery. The model's accuracy was evaluated based on the results obtained, yielding two evaluation metrics, RMSE = 23.70 and $R^2 = 0.82$.

Power System Technology
ISSN:1000-3673
Received: 16-01-2024 Revised: 12-02-2024 Accepted: 07-03-2024

In [36] 2015, for the prediction of NO_X and Soot levels in a four-cylinder Mercedes-Benz OM355 engine, a combination of Artificial Neural Network (ANN) and Ant Colony Optimization (ACO) algorithms was utilized. The data collected to test and verify the proposed model included measurements and recordings of various parameters at different engine speeds and power levels. The model's accuracy was assessed based on the results obtained, yielding two evaluation metrics, MSE = 0.0028 and R^2 = 0.911.

III. THE PROPOSED ALGORITHM

This section will provide a detailed description of the dataset collected for this study. Subsequently, the preprocessing steps performed on this data will be examined. Following that, the overall structure and specific details about the CNN and LSTM models will be discussed. Finally, the proposed Predictive DCNN model, a fusion of the CNN and LSTM models, will be presented.

A. *DataSet*

In this section, data intended for input into the proposed DCNN model is derived from a dual-fuel ignition compression engine. All performance tests and emissions measurements about pollutants were conducted at the Research and Development Center of Engine Manufacturers in Tabriz, Iran. The researchers in this study had previously concentrated on the prospect of employing Compressed Natural Gas (CNG) in a four-cylinder ignition compression engine, with CNG serving as the primary fuel and diesel fuel as the secondary ignition [18]. An investigation was conducted to evaluate the feasibility of employing this dual-fuel configuration in an ignition compression engine without utilizing an SI system and to compare variables such as engine output power and the emission levels from combustion. The primary aim of utilizing CNG to provide the primary portion of engine power was the reduction of pollutants, including Carbon Monoxide (CO), Nitrogen Oxides (NO_X), Hydrocarbons (HC), Carbon Dioxide (CO_2), Oxygen (O_2), and Soot, when compared to using diesel fuel alone. This study gathered data for the training and validation of the proposed model over a standard time cycle of 10 minutes (10 minutes). All functional tests, which encompassed the measurement and recording of pollutants and input parameters, were executed while the engine was operating at five distinct rotational speeds: 1200 rpm, 1400 rpm, 1600 rpm, 1800 rpm, and 2000 rpm, with three repetitions for each speed level. At each five-second interval within the specified time frame (10 minutes), 11 parameter values were measured and recorded by physical sensors. After each repetition, 120 new values were acquired for each parameter, culminating in 360 values after conducting all three repetitions. Considering the five different speed levels, 1800 data points were collected and documented in the designated dataset. The parameters utilized in this dataset are presented in Table 1.

Table 1. Collected Parameters for the Dataset

Parameter name	Unit
Speed	rpm
Torque	N.m
Intake Air Flow	Kg.h-1
Pre-Injection Timing	^oCA

Power System Technology
ISSN:1000-3673
Received: 16-01-2024 Revised: 12-02-2024 Accepted: 07-03-2024

Pre-Injection Quantity	Kg.h-1
Total Fuel Injection Quantity	Kg.h-1
Fuel Temperature	°C
Fuel Pressure	bar
Atmospheric Temperature	°C
Atmospheric Humidity	%
NOx	ppm

The relevant values for 11 parameters for the proposed DCNN model simulation have been gathered and recorded. Among these parameters, NO_X emissions (in mol/s) are chosen as the output parameter for the predictive model. The input parameters for the analysis of the proposed model include velocity (m/s), torque (N·m), fuel pressure (Pa), fuel temperature (K), input flow (m^3/s), pre-injection timing (s), pre-injection quantity (mol), total fuel injection amount (mol), fuel temperature (K), fuel pressure (Pa), atmospheric temperature (K), and atmospheric humidity (in %). The NO_X emissions level was measured using an AVL 415S pollutant analyzer, while the other input parameters were measured using a SCHENCK dynamometer model W230 and recorded. The dataset comprises 1800 data points, with all parameters obtained from a dual-fuel ignition compression engine under five different rotational speeds in three consecutive repetitions.

B. Data PreProcessing

Given the large number of input parameters recorded in the initial data collection and the absence of a meaningful relationship between some of these input parameters and the generation of NO_X emissions, it is necessary to analyze each input parameter separately to determine the essential level of correlation. Correlation refers to the relationship between two or more quantities, and the correlation coefficient quantifies the numerical value of this relationship. By removing parameters with lower correlations, the model's dimensions can be effectively reduced, thereby increasing its accuracy. In this section, the Spearman correlation coefficient is used for the separate analysis of pre-selected input parameters. The Spearman correlation coefficient can indicate the extent of nonlinear correlation between parameters and reveal any relationship between quantities. The Spearman correlation coefficient test is non-parametric and typically assesses the relationship between quantitative and ranked data. Since this correlation coefficient is non-parametric, it can usually be applied without considering the normality of observations. In summary, when the sample size is small, and the assumption of normality is unreasonable, the Spearman correlation coefficient is employed. The equation related to the Spearman correlation coefficient is represented by equation (1).

$$\rho = \frac{\sum_{i=1}^{n} x_i^2 - \frac{1}{2}\sum_{i=1}^{n}(x_i - y_i)^2}{\sum_{i=1}^{n} x_i^2} = 1 - \frac{\sum_{i=1}^{n}(x_i - y_i)^2}{2\sum_{i=1}^{n} x_i^2} = 1 - \frac{6\sum_{i=1}^{n}(x_i - y_i)^2}{n(n^2-1)} = 1 - \frac{6\sum_{i=1}^{n} d_i^2}{n(n^2-1)} \quad (1)$$

In the above expression, "n" represents the total number of samples, and d_i^2 denotes the squared difference in the rank of two variables after sorting the x_i values, where d_i is defined

Power System Technology
ISSN:1000-3673
Received: 16-01-2024 Revised: 12-02-2024 Accepted: 07-03-2024

as $d_i = (x_i - y_i)$. The parameter "input" pertains to the correlation and y_i represents the value of NO_X. The positive values obtained from this expression indicate a positive correlation between the two parameters, signifying a co-directional change. Conversely, negative values indicate a negative correlation between the two parameters, implying an inverse trend relationship. When the absolute value of the correlation coefficient approaches one, it indicates a more robust correlation and a more impactful relationship between the parameters. In contrast, when the absolute value of the correlation coefficient approaches zero, it signifies a weaker correlation and a relationship with lower influence.

Based on the results obtained from the correlation analysis between input parameters and NO_X as an output parameter, critical parameters for use in the proposed deep model training process were selected. The correlation levels between three parameters—fuel temperature (T_f), atmospheric temperature (T_a), and atmospheric humidity (RH_a)—and NO_X emissions were found to be minimal. Therefore, they can be excluded due to the low correlation coefficients between these three parameters and NO_X emissions. Additionally, the parameter representing the pre-injection quantity with NO_X emissions exhibited a significant nonlinear correlation, making it a candidate as one of the input variables for the proposed DCNN model.

In summary, after completing the data correlation-related preprocessing, three input parameters, fuel temperature (T_f), atmospheric temperature (T_a), and atmospheric humidity (RH_a), were removed, while the remaining input parameters were retained for training the model.

Once the input and output parameters of the proposed model have been defined, the next step in this process involves normalizing these parameters. Data normalization theory entails standardizing each input variable through a mathematical operation, initially constraining the input variable's range of variation between 0 and 1. This mathematical operation is illustrated in equation (2), where X represents the value of each input parameter, X_{min} and X_{max} are the minimum and maximum values of the input and X_n is the standardized output.

$$X_n = \frac{X - X_{min}}{X_{max} - X_{min}} \quad (2)$$

By mapping values to the range [0, 1], data normalization prevents excessive prediction errors and facilitates faster model convergence.

C. CNN Model

CNNs are a type of neural network that exhibits higher complexity than classical artificial neural network methods. A CNN comprises three main layers: the convolutional layer, the pooling layer, and the fully connected layer. CNNs typically employ the specific rules defined in equations (3) and (4) to implement forward and backward error propagation neural networks.

$$x_j^{L+1} = \sum_i w_{j,i}^{L+1} x_i^L \quad (3)$$

$$g_i^L = \sum_j w_{j,i}^{L+1} g_j^{L+1} \quad (4)$$

In equations (3) and (4), x_j^L and g_i^L represent the activation and gradient of unit i in layer L, respectively. $w_{j,i}^{L+1}$ denotes the weight connection from unit i in layer L to unit j in layer $L+$

Power System Technology
ISSN:1000-3673
Received: 16-01-2024 Revised: 12-02-2024 Accepted: 07-03-2024

1, which can be observed as activation units in the higher layer, activating all connected units to them. Similarly, units in the lower layer encompass gradients from all connected units to them. The strategy for computing gradients in a CNN implementation is somewhat intricate. Due to border effects, this complexity arises because the number of connections leaving each unit is not constant in a convolutional layer.

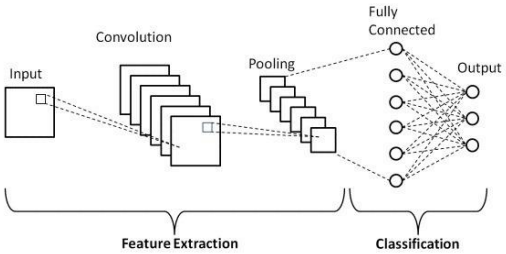

Figure 1. The Convolutional Neural Network Architecture

Figure 1 illustrates the architecture of a CNN. This type of neural network is one of the variants of deep learning networks inspired by the Perceptron neural network. CNNs typically come in three types: one-dimensional CNNs, two-dimensional CNNs, and three-dimensional CNNs.

In the first type, the CNN kernel moves in one direction. One-dimensional CNNs are commonly used for time series data. In the second type, the kernels move in two directions. Two-dimensional CNNs find applications in image labeling and processing. The third type employs kernels that move in three directions. Researchers utilize this type of CNN for three-dimensional data, such as CT scans and MRI images.

This deep network consists of an input layer, an output layer, and a deep hidden layer. The network's hidden layer comprises individual layers that define the system's architecture. Notable architectural designs include LeNet, GoogLeNet, and AlexNet. In essence, the hidden layer of a CNN encompasses a specific arrangement of numerical layers.

The convolutional layer is a fundamental component of a CNN, and its output can be conceptualized as a three-dimensional array of neurons arranged in three dimensions. Consequently, the output of this cube will also be a three-dimensional array. Each of these neurons is connected to a region of the previous layer, depending on the size of the convolutional layer's filter. For example, if a filter with a size of (3,3) is used, a neuron at position [x, y, z] will be connected to all neurons in the previous layer with horizontal and vertical positions relative to it. Hyperparameters control the size of the output volume, with depth, stride, and zero-padding being essential types of these hyperparameters. Depth is a parameter that can be chosen, and it controls the number of neurons connected to a region in the input volume in the convolutional layer. Stride should be specified by the depth columns defined around spatial dimensions (width and height). In the case of stride, the most common value is one. When the stride equals one, a new depth column of neurons is assigned to spatial coordinates with only a one-unit spatial distance from each other. This creates a receptive field with a significant overlap between columns, making the output volume larger.

Conversely, taking longer strides will result in a receptive field with less overlap, and the output volume will be smaller regarding spatial dimensions. Sometimes, it is more convenient

Power System Technology
ISSN:1000-3673
Received: 16-01-2024 Revised: 12-02-2024 Accepted: 07-03-2024

to pad the input volume with zeros around its edges. In other words, the border of the input matrix is filled with zeros. Padding or zero-padding adds extra pixels outside the matrix, and adding zeros means that the value of each added pixel is zero.

In CNN architecture, it is common practice to incorporate a pooling layer periodically. Typically, this layer is used to reduce the spatial size of the network and mitigate overfitting errors. This operation is performed separately on each depth, employing various pooling layers. Max Pooling, Sum Pooling, and average pooling are used in CNNs. The Max Pooling function is most commonly used, as exemplified in Figure 2. This function is a nonlinear operation. Each neuron's output represents the maximum value within a small input region, which depends on the filter size. Pooling layers can have a stride more significant than one. This is important because it reduces the computational requirements, memory usage, and the number of parameters that need to be learned in consecutive layers. This spatial reduction also allows the units in subsequent layers to be influenced by a larger region of the original image.

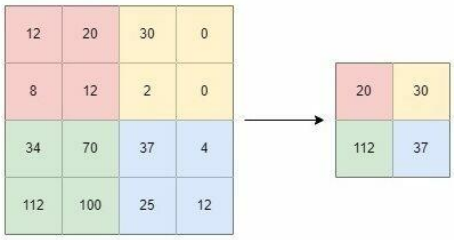

Figure 2. An Example of a Max Pooling Layer

In deep models, nonlinear activation functions are typically employed. The output signal will be a simple linear function if the activation function is not applied to the system. A linear function is a first-degree polynomial. Solving a linear equation is straightforward; it has limited complexity and less capability to learn complex functional behaviors from data. This layer performs a simple, practical element in the model and preserves the layer size without the need for any statistical parameters. Several commonly used activation functions (Sigmoid, Rectified Linear Unit (ReLU), and Leaky ReLU), along with their two-dimensional graphs and equations, are presented in Table 2. The ReLU function is the most widely used in CNNs due to its facilitation of the training process.

Table 2. Several Commonly Used Activation Functions

Function Name	Equation	The Chart
Sigmoid	$f(x) = \sigma(x) = \frac{1}{1+e^{-x}}$	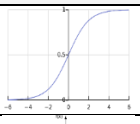
ReLU	$f(x) = \begin{cases} 0 & x < 0 \\ x & x \geq 0 \end{cases}$	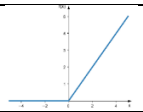
Leaky ReLU	$f(x) = \begin{cases} 0.01x & x < 0 \\ x & x \geq 0 \end{cases}$	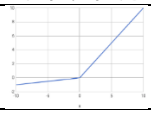

Power System Technology
ISSN:1000-3673
Received: 16-01-2024 Revised: 12-02-2024 Accepted: 07-03-2024

In a CNN, the feedforward algorithm is used for network training. The Back-Propagation (BP) method is also employed for error computation, enabling the modular presentation and debugging of neural networks. The training procedure unfolds as follows: initially, the first layer undergoes training as an autoencoder, wherein the objective function is minimized with training sets as inputs. Subsequently, the second layer is likewise trained as an autoencoder, taking the output of the first layer as its input. This process continues for the desired number of layers. The output of the final layer serves as input for the prediction layer, with its parameters being initialized randomly and refined through supervised training. Precise parameter adjustments for all layers are accomplished using the BP method.

D. LSTM Model

LSTM is an improved version of the Recurrent Neural Network (RNN) that facilitates the retention of past data in memory, addressing the vanishing gradients that plague traditional RNNs. LSTM suits classification, processing, and time-series prediction tasks in uncertain temporal delays. This model also employs the BP method during the training process. The architecture of an LSTM network is depicted in Figure 3.

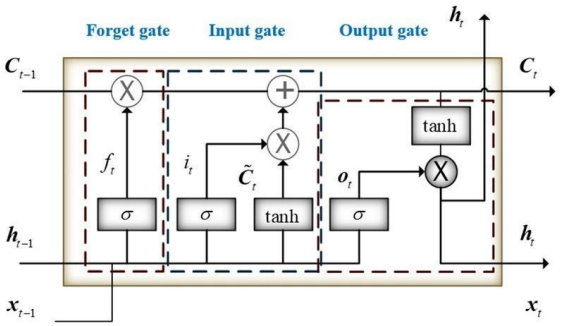

Figure 3. The Long Short-Term Memory Architecture

The above figure has three inputs (x, h, and c). x represents the input at a time (sequence) t. Similar to a simple RNN, h is the "Hidden State" obtained from the previous time step (previous sequence) as memory. Input c is a "Cell State" that regulates which information from previous long sequences should influence the current block. For a better understanding, an LSTM block can be divided into three main sections: the "forget gate," the "gate input," and the "gate output."

The forget gate determines which details should be discarded from the block. The sigmoid function makes this decision. The sigmoid function looks at the previous state (ht-1) and the input content (Xt) and returns an output value between 0 (discard) and 1 (retain) for each number in the cell state Ct-1. The gate input identifies which input values should be used to improve memory. The sigmoid function decides which values should pass between 0 and 1. The tanh function passes the values and assigns weights from -1 to 1 based on their importance. The gate output utilizes the input and memory of the block to make decisions regarding the output. The sigmoid function determines which values should pass between 0 and 1. The tanh function passes the values based on their importance, assigns weights in the range of -1 to 1, and multiplies them with the output of the sigmoid function.

Power System Technology
ISSN:1000-3673
Received: 16-01-2024 Revised: 12-02-2024 Accepted: 07-03-2024

E. DCNN Proposed Model

The DCNN model introduced in this study is derived from the fusion of two models: CNN and LSTM. This model leverages the capabilities of CNN for feature extraction and the capabilities of LSTM for time-series prediction. The details of this proposed deep model are presented in the following sections.

Input Data

The input data for the model is obtained during the initial data collection stage. Data preprocessing is performed with a stride of one. Processed data from the engine parameters and pollutants are used as inputs to the model for extracting spatial features. The preprocessed data is divided into training, testing, and verification. 75% of the data is allocated to the training process, 10% to the testing process, and 15% to the verification process.

Feature Extraction and Model Training

As previously mentioned, 1D CNN can project data variables into a high-dimensional space with a high-dimensional map and extract local features based on spatial and temporal correlations. In 1D CNN, matrix multiplication performs convolution calculations on time series data. This type of CNN is highly suitable for processing time series data recorded by sensors. Since emissions data from dual-fuel ignition compression engines consist of emissions time series recorded by sensors, 1D CNN can effectively extract features from emissions data and improve the model's prediction accuracy.

During the CNN architecture debugging process, the model may suffer from underfitting if the convolution layers are too low due to insufficient feature extraction capabilities. Conversely, if the number of convolution layers is excessively high, it can lead to overfitting issues. While pooling layers can somewhat mitigate the problem of overfitting, excessive use of pooling layers can also reduce the dimensionality of input features for the LSTM network.

This reduction can potentially harm the extraction of time series features by LSTM and consequently decrease the performance of network connections. Through multiple iterations for CNN debugging processes, a proposed structure with four convolutional layers, a maximum pooling layer, and a fully connected flat layer for the first part of the recommended deep model was selected. At this stage, the training dataset, which includes seven input features and one output label, is fed into a 1D-CNN for feature extraction and undergoes four convolution operations. Following the convolution operations, a ReLU activation function maps the features to nonlinear intervals in a high-dimensional space. Subsequently, a maximum pooling layer (Max Pooling) is also employed to reduce the output dimensions. The number of convolution kernels is set at 16, 32, 64, and 128, respectively. The kernel sizes for each pair of convolutional layers and pooling are configured as 1×3 with a stride of one. After completing three consecutive convolution operations and one Max pooling operation, a feature matrix with dimensions of 28*16 is obtained. This matrix is flattened into a one-dimensional vector of length 2048 and applied as input to the LSTM model.

To ensure an increase in the precision of the proposed deep model, hyperparameters are optimized using the grid search method and applied to the input LSTM. This approach divides the search space into a grid and systematically examines all intersections. The best combination of hyperparameters can be determined by evaluating the results from these intersections. In this stage, the search range for hyperparameters for LSTM is determined, and this range is then applied to the grid search function to organize all possible combinations within the specified

Power System Technology
ISSN:1000-3673
Received: 16-01-2024 Revised: 12-02-2024 Accepted: 07-03-2024

range. The hyperparameter search range in the LSTM structure ranges from 1 to 10 for depth, 10 to 200 for the number of neurons in the hidden layers, and 10 to 300 for the Batch Size (BC).

The LSTM structure in the proposed deep model consists of an input layer, two hidden layers (40 neurons for each layer), an output layer, and a fully connected layer. LSTM repeatedly trains the gate input, forget gate, and gate output to adjust their respective hyperparameters. After completing the training process following 50 epochs, the final values for depth, the number of neurons in the hidden layers, and BC are determined as 2, 40, and 100, respectively. The number of iterations for the training and verification process of the model is set at 50 epochs.

The final hyperparameters for the proposed model are obtained through iterations and continuous optimization of different combinations of hyperparameters using the grid search function. Details related to the hyperparameters used in the proposed DCNN model are displayed in Table 3.

Table 3. Hyperparameters used in the proposed DCNN model

Hyperparameter name	Value
The number of convolution layers	4
The number of Pooling layers	1
Activator function	ReLU
The number of convolution kernels	16, 32, 64, 128
The size of the kernels	1×3
Learning rate	0.001
Stride	1
depth	2
The number of hidden layer neurons	40
Epochs	50
Optimization function	AdaptAhead
Loss Function	Binary Cross Entropy
Optimization Hyperparameters	Grid Search

F. Optimization Using the AdaptAhead Algorithm

The feature vectors extracted through DCNN training have been provided, and the network weights at each stride are updated by the AdaptAhead algorithm [37]. The initial learning rate is set to 0.001. The weights and biases of each neuron are continuously updated using this algorithm, which ultimately leads to the optimal output of the loss function. A total of 50 epochs are considered for the training and verification process of the model. By defining an objective function for the algorithm, an attempt is made to calculate the values of adjustable parameters in a way that minimizes the desired objective function concerning the test dataset.

Power System Technology
ISSN:1000-3673
Received: 16-01-2024 Revised: 12-02-2024 Accepted: 07-03-2024

IV. EXPERIMENTAL RESULTS

A. *Experimental Equipment and Setup*

The dual-fuel ignition compression engine (MT440C model) utilized in this study is a four-cylinder engine manufactured by Tabriz Engine Manufacturers, complying with national emission standards. The maximum brake power of this engine at a specific rotational speed of 2000 Revolutions per Minute (RPM) is 82 Brake Horse Power (BHP). In the dual-fuel mode, CNG is the primary fuel, and Euro 4 standard diesel is the ignition-assisting fuel. Additional technical specifications of this engine are presented in Table 4.

Table 4. Technical Specifications of the Dual-Fuel Ignition Compression Engine (MT440C Model)

Specifications	Value	Unit
Number of cylinders	4	inline
Bore	100	mm
Stroke	Mm127	mm
Cubic Capacity	3.99	liters
Compression Ratio	17.5:1	-
Electrical System	12	v
Induction System	-	Turbocharged
Combustion System	-	Direct Injection
Max Torque	332	N.m
Max Power	61	kw
Max Speed	2000	rpm
Weight	378	kg

The schematic representation of the engine's functional and emissions performance testing components is depicted in Figure 4, while the physical configuration of the engine used is illustrated in Figure 5.

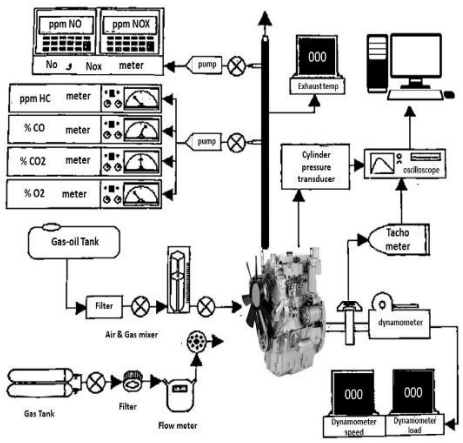

Figure 4. Schematic Diagram of Engine Performance and Emissions Testing Components

Power System Technology
ISSN:1000-3673
Received: 16-01-2024 Revised: 12-02-2024 Accepted: 07-03-2024

Figure 5. Physical Configuration of the Dual-Fuel Ignition Compression Engine (MT440C Model)

For measuring the pollutants resulting from engine combustion during testing, an AVL 415S emissions analyzer device was employed. This device, produced by AVL Ditest in Germany, can digitally display the emissions of spark-ignition and compression-ignition automotive engines, including NO_X, HC, CO, O_2, and CO_2, in the exhaust gas output. In this study, the exhaust gas from the engine was transferred to the AVL 415S emissions analyzer through a conduit, where NO_X emissions were measured separately in real-time. Other parameters required for the input dataset of the proposed DCNN model were measured and recorded using a Schenck dynamometer model W230. This German-made dynamometer, utilizing eddy current technology, boasts a maximum power of 230 KW, a maximum speed of 7500 rpm, and a maximum torque of 750 N.m. A mechanical flow meter was also employed to measure the consumption rate of CNG. The flow meter used in this study was of the orifice type and could measure flow rates from 1/ to 16 m^3/h.

B. The Simulation Environment

To simulate the proposed deep learning model, a computer system with an Intel(R) Core(TM) i7-6500U CPU @ 2.50 GHz 2.59 GHz processor, 8 gigabytes of RAM, an NVIDIA GeForce 940M graphics processor, and the Python programming language were utilized. The model development was conducted using the Python language with the assistance of the Keras library and the TensorFlow backend. The following code snippet represents a part of the process related to model construction and the selection of the optimization algorithm:

```
DCNN = Model (input_data, x)
DCNN.compile (optimizer= Adaptahead, loss='binary_crossentropy')
```

In the code snippet above, the "Model" command is used to create the model, with "input_data" selected as the input layer and "x" as the final output layer. After constructing the model, it must be compiled. The "Compile" command is employed for executing and compiling the model, with the desired parameters for selecting the optimization algorithm and the cost function. The "optimizer" parameter is used to choose the optimization function, and the "loss"

Power System Technology
ISSN:1000-3673
Received: 16-01-2024 Revised: 12-02-2024 Accepted: 07-03-2024

parameter is employed to select the cost function. In this work, the "AdaptAhead" algorithm is chosen as the optimization algorithm, and the "binary_crossentropy" function is selected as the cost function. It is worth noting that continuous monitoring of the model's performance accuracy for verification data is necessary during training. To prevent overfitting and terminate the training process when no improvement in accuracy is observed within an epoch, the training process should be monitored closely. The following code snippet is related to initiating the training process of the model:

```
n_epocks = 50
n_batch_size = 100
DCNN.fit (
        x_train,
        epochs = n_epochs,
        batch_size = n_batch_size,
        shuffle = True,
        validation_data = (x_test_val)
      )
```

In the code snippet above, the number of strides or epochs and the BC are first specified before entering the model training phase. Epochs represent the number of stages in which the model sees all the data. This work considers 50 epochs and a BC of 100, and the training process begins with the "fit" command. The "shuffle" parameter changes the data arrangement, effectively shuffling the data. Setting this parameter to "True" ensures that the model avoids the influence of data sequence on the results. The last parameter, "Validation," pertains to prediction data. In this section, the evaluation dataset can be used to predict the NO_X emissions values for the dual-fuel CI engine. At the end of each training round, the model is provided with the evaluation data (x_test_val), which is related to the evaluation data, to present results on these data, allowing for a more realistic assessment of the outcomes.

C. Evaluation Criteria

To evaluate the performance of the proposed DCNN model, this study employs four key indicators commonly used for assessing the proper functioning of neural networks. These four indicators include Mean Absolute Error (MAE), RMSE, R^2, and Mean Absolute Percentage Error (MAPE). R^2 is typically considered between zero and one. The accuracy estimation of the proposed model by these four indicators is presented in equations (5), (6), (7), and (8), respectively. In all the following equations, n represents the total number of samples, y_a^i denotes the actual value, y_p^i represents the predicted value and y_b^i signifies the mean of actual responses.

$$(5) \quad MAE = \frac{1}{n}\sum_{i=1}^{n}\left|y_a^i - y_p^i\right|$$

$$(6) \quad \mathrm{RMSE} = \sqrt{\frac{1}{n}\sum_{i=1}^{n}\left(y_a^i - y_p^i\right)}$$

$$(7) \quad MAPE = \frac{1}{n}\sum_{i=1}^{n}\left|\frac{y_a^i - y_p^i}{y_b^i}\right| \times 100\ \%$$

$$(8) \quad R^2 = 1 - \frac{\sum_{i=1}^{n}(y_a^i - y_p^i)^2}{n\sum_{i=1}^{n}(y_a^i - y_b^i)^2}$$

Power System Technology
ISSN:1000-3673
Received: 16-01-2024 Revised: 12-02-2024 Accepted: 07-03-2024

D. Output Results

The proposed DCNN model was evaluated using various verification metrics after training. The average results for the MAE, RMSE, R^2, and MAPE metrics are presented in Table 5.

Table 5. Evaluation criteria amount for the Proposed DCNN Model

The Proposed DCNN Model	
Evaluation Criteria	**Amounts**
MAE	6.613
RMSE	21.708
R^2	0.997
MAPE	12.194

Ten tests were conducted for each evaluation metric to obtain precise values and eliminate random errors. Some of the results from these tests for the RMSE and R^2 metrics are shown in Table 6. Based on the obtained results, it can be concluded that the proposed DCNN model exhibited high accuracy in predicting NO_X emissions with an average RMSE of 21.70 and an R^2 of 0.997.

Table 6. Model Accuracy Evaluation Using RMSE and R^2 Metrics (Ten Repetitions)

Test Number	**Evaluation criteria**	
	RMSE	**R^2**
1	20.8820	0.9623
2	20.2389	0.9760
3	20.8374	0.9667
4	24.5900	0.9958
5	21.9463	0.9714
6	25.4446	0.9830
7	20.9647	0.9948
8	21.1579	0.9952
9	20.9959	0.9928
10	21.7089	0.9973

A portion of the results related to the prediction of NO_X emissions from dual-fuel CI engines in real-state conditions and the predictions made by the proposed DCNN model at different time strides are presented in Table 7.

Table 7. NO_X emissions prediction in real state conditions and predictions by the proposed DCNN model

Parameters		**Values**				
Time (s)	**Speed (rpm)**	1200	1400	1600	1800	2000

Power System Technology
ISSN:1000-3673
Received: 16-01-2024 Revised: 12-02-2024 Accepted: 07-03-2024

in seconds (25)	Real NO_X	2100	1800	1690	1700	1570
	Predicted NOX	2011	1830	1670	1690	1535
in seconds (40)	Real NO_X	2200	1960	1700	1820	1500
	Predicted NO_X	2331	1909	1798	1790	1500
in seconds (65)	Real NO_X	2890	2100	1700	1798	1360
	Predicted NO_X	2737	2064	1009	1780	1325
in seconds (120)	Real NO_X	2120	1850	1740	1720	1610
	Predicted NO_X	2021	1800	1690	1650	1620

Table 8 compares the proposed model with some recent studies in NO_X emissions prediction. The results from this table indicate that the proposed DCNN model outperformed the methods introduced in previous works.

Table 8. Comparison of the proposed DCNN Model with related works

#No	Reference	Year	Evaluation criteria	
			RMSE	R^2
1	-	-	21.70	0.99
2	[30]	2023	33.49	0.97
3	[31]	2022	-	0.92-0.95
4	[32]	2022	70.06	-
5	[33]	2021	46.11	0.98
6	[34]	2020	68	-
7	[35]	2020	23.70	0.82
8	[36]	2015	-	0.91

V. CONCLUSIONS AND FUTURE WORKS

This study proposes a DCNN model for predicting NO_X emissions from a dual-fuel CI engine. The proposed DCNN model, with the selection of optimal hyperparameters, extracts important features using CNN capabilities and establishes relationships between different time series using LSTM capabilities. A dataset is prepared to train the proposed model by selecting important and influential features related to NO_X emissions from the dual-fuel CI engine (MT440C model). Data collection is performed by measuring and recording the values of input parameters to the engine and the level of NO_X emissions within a standard time interval. Some initial data preprocessing is carried out to prepare it for the training process. The pooling capabilities of the CNN and LSTM models enable the proposed model to uncover the complex

Power System Technology
ISSN:1000-3673
Received: 16-01-2024 Revised: 12-02-2024 Accepted: 07-03-2024

relationships among transient emissions data features, thereby improving the accuracy of NO_X emissions prediction from the dual-fuel CI engine. The performance of the proposed model is evaluated using various metrics. The results of this evaluation, with RMSE = 21.70 and R^2 = 0.997, demonstrate the high accuracy of NO_X emissions prediction by the DCNN model compared to previous work in this field.

As a future research direction, various datasets can be employed on different engines to investigate the performance of the proposed method. Moreover, exploring other architectures used in deep learning or testing them for optimizing various meta-heuristic algorithms is possible.

REFERENCES

[1] Al-Abadi, N. J. A., & Al-Qatrani, R. I. N. (2023). Prospects for Future Competition Between Renewable Energy Sources and Fossil Fuels in the Global Energy Markets Basra University of Oil and Gas. *Migration Letters*, *20*(S2), 679-699.

[2] Olujobi, O. J., Okorie, U. E., Olarinde, E. S., & Aina-Pelemo, A. D. (2023). Legal responses to energy security and sustainability in Nigeria's power sector amidst fossil fuel disruptions and low carbon energy transition. *Heliyon*, *9*(7).

[3] Matallah, S., Boudaoud, S., Matallah, A., & Ferhaoui, M. (2023). The role of fossil fuel subsidies in preventing a jump-start on the transition to renewable energy: Empirical evidence from Algeria. *Resources Policy*, *86*, 104276.

[4] Bhagat, R. N., Sahu, K. B., Ghadai, S. K., & Kumar, C. B. (2023). A review of diesel engine performance and emissions operating on dual fuel mode with hydrogen as a gaseous fuel. *International Journal of Hydrogen Energy*.

[5] Bhagat, R. N., Sahu, K. B., Ghadai, S. K., & Kumar, C. B. (2023). A review of performance and emissions of diesel engine operating on dual fuel mode with hydrogen as gaseous fuel. *International Journal of Hydrogen Energy*.

[6] Palani, Y., Devarajan, C., Manickam, D., & Thanikodi, S. (2022). Performance and emission characteristics of biodiesel-blend in diesel engine: A review. *Environmental Engineering Research*, *27*(1).

[7] Arefin, M. A., Nabi, M. N., Akram, M. W., Islam, M. T., & Chowdhury, M. W. (2020). A review on liquefied natural gas as fuels for dual fuel engines: Opportunities, challenges and responses. *Energies*, *13*(22), 6127.

[8] Pedrozo, V. B., Wang, X., Guan, W., & Zhao, H. (2022). The effects of natural gas composition on conventional dual-fuel and reactivity-controlled compression ignition combustion in a heavy-duty diesel engine. *International Journal of Engine Research*, *23*(3), 397-415.

[9] Vedharaj, S. (2021). Advanced ignition system to extend the lean limit operation of spark-ignited (SI) engines—A review. *Alternative Fuels and Advanced Combustion Techniques as Sustainable Solutions for Internal Combustion Engines*, 217-255.

[10] Thiyagarajan, S., Varuvel, E., Karthickeyan, V., Sonthalia, A., Kumar, G., Saravanan, C. G., ... & Pugazhendhi, A. (2022). Effect of hydrogen on compression-ignition (CI) engine fueled with vegetable oil/biodiesel from various feedstocks: A review. *International Journal of Hydrogen Energy*, *47*(88), 37648-37667.

Power System Technology
ISSN:1000-3673

Received: 16-01-2024 Revised: 12-02-2024 Accepted: 07-03-2024

[11] Salam, S., Choudhary, T., Pugazhendhi, A., Verma, T. N., & Sharma, A. (2020). A review on recent progress in computational and empirical studies of compression ignition internal combustion engine. *Fuel*, *279*, 118469.

[12] Kalghatgi, G. (2019). Development of fuel/engine systems—the way forward to sustainable transport. *Engineering*, *5*(3), 510-518.

[13] Arefin, M. A., Nabi, M. N., Akram, M. W., Islam, M. T., & Chowdhury, M. W. (2020). A review on liquefied natural gas as fuels for dual fuel engines: Opportunities, challenges and responses. *Energies*, *13*(22), 6127.

[14] Vinoth Kanna, I., Arulprakasajothi, M., & Eliyas, S. (2021). A detailed study of IC engines and a novel discussion with comprehensive view of alternative fuels used in petrol and diesel engines. *International Journal of Ambient Energy*, *42*(15), 1794-1802.

[15] Nayak, S. K., Le, H. S., Kowalski, J., Deepanraj, B., Duong, X. Q., Truong, T. H., ... & Nguyen, P. Q. P. (2023). Performance and emission characteristics of diesel engines running on gaseous fuels in dual-fuel mode. *International Journal of Hydrogen Energy*.

[16] Hollevoet, L., Vervloessem, E., Gorbanev, Y., Nikiforov, A., De Geyter, N., Bogaerts, A., & Martens, J. A. (2022). Energy-Efficient Small-Scale Ammonia Synthesis Process with Plasma-enabled Nitrogen Oxidation and Catalytic Reduction of Adsorbed NOx. *ChemSusChem*, *15*(10), e202102526.

[17] Kumar, A., Rana, S., Wang, T., Dhiman, P., Sharma, G., Du, B., & Stadler, F. J. (2023). Advances in S-scheme heterojunction semiconductor photocatalysts for CO2 reduction, nitrogen fixation and NOx degradation. *Materials Science in Semiconductor Processing*, *168*, 107869.

[18] Niknam, Y., Zamani, D. M., & Pareshkoohi, M. G. (2023). Converting Compression Ignition Engine to Dual Fuel (Diesel+ CNG) Engine and Experimentally Investigating its Performance and Emissions.

[19] Zhang, Q., Xiao, J., Tian, C., Chun-Wei Lin, J., & Zhang, S. (2023). A robust deformed convolutional neural network (CNN) for image denoising. *CAAI Transactions on Intelligence Technology*, *8*(2), 331-342.

[20] Sasaki, H., Hidaka, Y., & Igarashi, H. (2021). Explainable deep neural network for design of electric motors. *IEEE Transactions on Magnetics*, *57*(6), 1-4.

[21] Liu, Y., Pu, H., & Sun, D. W. (2021). Efficient extraction of deep image features using convolutional neural network (CNN) for applications in detecting and analysing complex food matrices. *Trends in Food Science & Technology*, *113*, 193-204.

[22] Gholamalinezhad, H., & Khosravi, H. (2020). Pooling methods in deep neural networks, a review. *arXiv preprint arXiv:2009.07485*.

[23] Shin, S., Lee, Y., Lee, Y., Park, J., Kim, M., Lee, S., & Min, K. (2022). Designing a steady-state experimental dataset for predicting transient NOx emissions of diesel engines via deep learning. *Expert Systems with Applications*, *198*, 116919.

[24] Ehsani Chimeh, H., & Karami, M. (2018). Spam Detection from Big Data based on Evolutionary Data Mining Systems. *Transactions on Machine Intelligence*, *1*(1), 1-9. doi: 10.47176/TMI.2018.1

Power System Technology
ISSN:1000-3673

Received: 16-01-2024 *Revised: 12-02-2024* *Accepted: 07-03-2024*

[25] Zamani, M., Azadi, S., & Rahmani Seryasat, O. (2021). Noise Reduction in Medical X-Ray Images Using Wavelet and Neural Networks. *Transactions on Machine Intelligence*, *4*(1), 36-52. doi: 10.47176/TMI.2021.36

[26] Ghayoumi Zadeh, H., Fayazi, A., Rahmani Seryasat, O., & Rabiee, H. (2022). A Bidirectional Long Short-Term Neural Network Model to Predict Air Pollutant Concentrations: A Case Study of Tehran, Iran. *Transactions on Machine Intelligence*, *5*(2), 63-76. doi: 10.47176/TMI.2022.63

[27] Hajigol Yazdi, E., & Fakhrzad, M. (2020). Supply Chain Risk Management by Risk Efficiency Index. *Transactions on Data Analysis in Social Science*, *2*(1), 23-35. doi: 10.47176/TDASS/2020.23

[28] Asgari, F., Sargazi, M., & Haji Molana, S. M. (2021). Material requirements planning with a fuzzy model. *Transactions on Data Analysis in Social Science*, *3*(1), 14-22. doi: 10.47176/TDASS/2021.14

[29] Seighali, M., & Moradi, M. (2022). Application of Liquidity Ratios in Predicting Corporate Financial Crisis; Comparison of Support Vector Machine Model and Neural Network in Cement Industry. *Transactions on Data Analysis in Social Science*, *4*(1), 1-8. doi: 10.47176/TDASS/2022.1

[30] Shen, Q., Wang, G., Wang, Y., Zeng, B., Yu, X., & He, S. (2023). Prediction Model for Transient NOx Emission of Diesel Engine Based on CNN-LSTM Network. *Energies*, *16*(14), 5347.

[31] Pillai, R., Triantopoulos, V., Berahas, A. S., Brusstar, M., Sun, R., Nevius, T., & Boehman, A. L. (2022). Modeling and predicting heavy-duty vehicle engine-out and tailpipe nitrogen oxide (NOx) emissions using deep learning. *Frontiers in Mechanical Engineering*, *8*, 11.

[32] Saif-Ul-Allah, M. W., Khan, J., Ahmed, F., Salman, C. A., Gillani, Z., Hussain, A., & Hasan, M. (2022). Computationally Inexpensive 1D-CNN for the Prediction of Noisy Data of NOx Emissions From 500 MW Coal-Fired Power Plant. *Frontiers in Energy Research*, *10*, 945769.

[33] Yu, Y., Wang, Y., Li, J., Fu, M., Shah, A. N., & He, C. (2021). A Novel Deep Learning Approach to Predict the Instantaneous NO_x Emissions from Diesel Engine. *Ieee Access*, *9*, 11002-11013.

[34] Li, N., & Hu, Y. (2020). The deep convolutional neural network for NOx emission prediction of a coal-fired boiler. *IEEE Access*, *8*, 85912-85922.

[35] He, W., Li, J., Tang, Z., Wu, B., Luan, H., Chen, C., & Liang, H. (2020). A novel hybrid CNN-LSTM scheme for nitrogen oxide emission prediction in FCC unit. *Mathematical Problems in Engineering*, *2020*, 1-12.

[36] Mohammadhassani, J., Dadvand, A., Khalilarya, S., & Solimanpur, M. (2015). Prediction and reduction of diesel engine emissions using a combined ANN–ACO method. *Applied Soft Computing*, *34*, 139-150.

[37] Hoseini, F., Shahbahrami, A., & Bayat, P. (2019). AdaptAhead optimization algorithm for learning deep CNN applied to MRI segmentation. *Journal of digital imaging*, *32*, 105-115.